



FORSCHUNGS- UND TESTZENTRUM FÜR
SOLARANLAGEN
Institut für Thermodynamik und Wärmetechnik
Universität Stuttgart



Test Report

Efficiency measurement on an infrared radiator

Test Report No.: 16SU079

Stuttgart, 25th July, 2016

Client: Rudolf KOLLER Ges.m.b.H.
Rudolf-Koller-Straße 1
3902 Vitis
AUSTRIA

Manufacturer: Rudolf KOLLER Ges.m.b.H.

Typ: CL-750

Year of production: 2016

Table of Contents

1 Introduction.....	3
2 Determination of the emissivity of the front and back side of the infrared radiator....	3
3 Determination of the electrical power consumption of the infrared radiator	4
4 Determination of the duration of the heating-up phase.....	4
5 Determination of the surface temperature of the infrared radiator using infrared thermography	6
6 Calculation of the different portions of the Radiation of the infrared radiator	11
7 Calculation of the radiated power and of the heat emitted by free convection.....	12
8 Test methods.....	13

1 Introduction

Subject of the investigation is an electrical radiation heater type CL-750 of the company Rudolf KOLLER Ges.m.b.H.

The scope of the investigation is:

1. The determination of the emissivity of the front and back side of the infrared radiator
2. The determination of the electrical power consumption of the infrared radiator
3. The determination of the duration of the heating-up phase
4. The determination of the surface temperature of the infrared radiator using infrared thermography
5. The calculation of the radiated power and of the heat emitted by free convection
6. The calculation of the radiation efficiency and the ratio of IR-C radiation

2 Determination of the emissivity of the front and back side of the infrared radiator

The determination of the emissivity of the surfaces was done on samples of coated steel plates with the measuring device OPTOSOL. Figures 1 and 2 show the samples delivered by the client. On the right side of the figures the single sided coated samples are shown, which were used for the measurements. The investigated samples are made from steel and are powder coated. For the front and back side plates with the same coating are used.

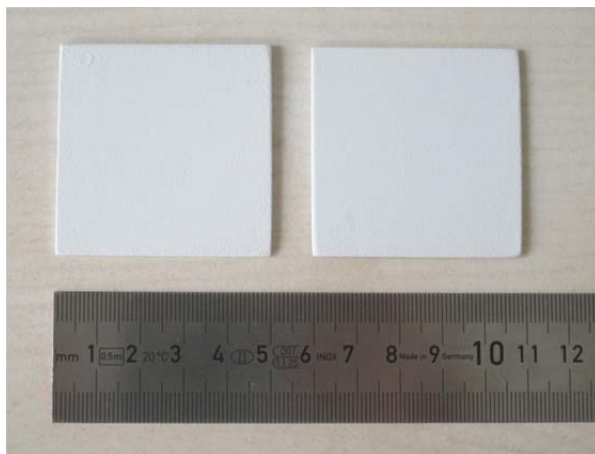


Figure 1: Coated steel plates front side

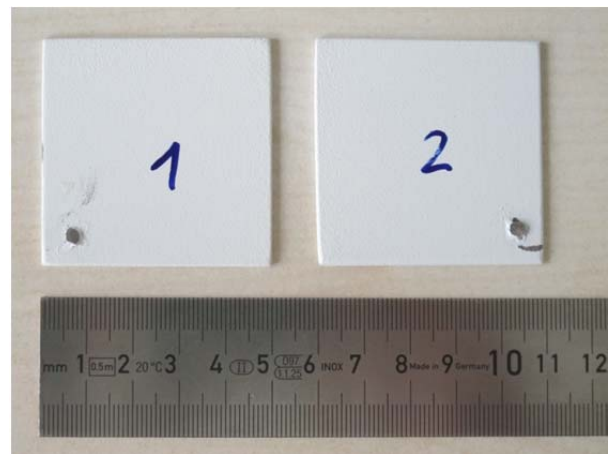


Figure 2: Coated steel plates back side

On each sample 20 measurements were carried out and the mean value was calculated.

The emissivity ϵ of the powder coated steel plate was determined to approx. 0.96.

This value was supplied to the thermography camera for the temperature calculation. With this value the temperatures determined with the thermography camera showed very good conformity with the temperature measured with the thermocouples placed on the surface (see also section 4).

3 Determination of the electrical power consumption of the infrared radiator

The electrical power consumption of the infrared radiator was measured during all thermography recordings as well as continuously during the determination of the heating-up phase with an active power meter. The electrical power consumption depends on the supply voltage. The range of the electrical power consumption was found to be between 558 W at 215 V~ and 592 W at 223 V~. During the determination of the heating-up phase the electrical power consumption was found to be between 580 W to 587 W and during the recording of the thermographs within this report between 576 W and 590 W with a mean value of 580 W.

4 Determination of the duration of the heating-up phase

For the determination of the heating-up phase 4 NiCr-Ni thermocouples were installed on the radiation heater, one in the upper right quarter on the front side, one on the lower right corner, one in the centre of the back side and one at the top right corner of the backside. These positions are representative for the maximum and minimum temperatures on the front and back side.

Figure 3 shows the front view of the radiation heater installed on the test rig by means of the installation kit supplied by the client. The thermocouples were fixed with temperature resistant aluminium adhesive tape to the surface and the measurement tip was glued to the surface using cyanoacrylate adhesive. To facilitate the spotting of the measuring points within the thermography additionally 2 aluminium tapes were placed adjacent to the measuring points. Using these temperature measuring points the temperatures determined with the thermography camera were checked.



Figure 3: Front side of the radiation heater with two temperature sensors

The temperature gradients at the measuring points after turning on the radiation heater are shown in figure 4. The heater was turned on at 13:26. The temperature rise in the centre of the front side takes place almost immediately and reaches after 35 min its maximum. The increase of the temperatures at the edge of the radiation heater is slower and hence the temperatures do not reach their maximum only after approx. 50 min. The heating-up phase in the centre of the back side lasts because of the heat insulation within the heater and the thermal conductivity of the steel plate approx. 75 min.

The heating-up phase takes approx. 45 min, since after this time the radiation heater emits its full radiation power at the front side.

The slight fluctuations of the temperatures after 45 min are due to small changes of the supply voltage. To determine the time constant the mean value of the temperatures from 14:20 to 15:00 was used.

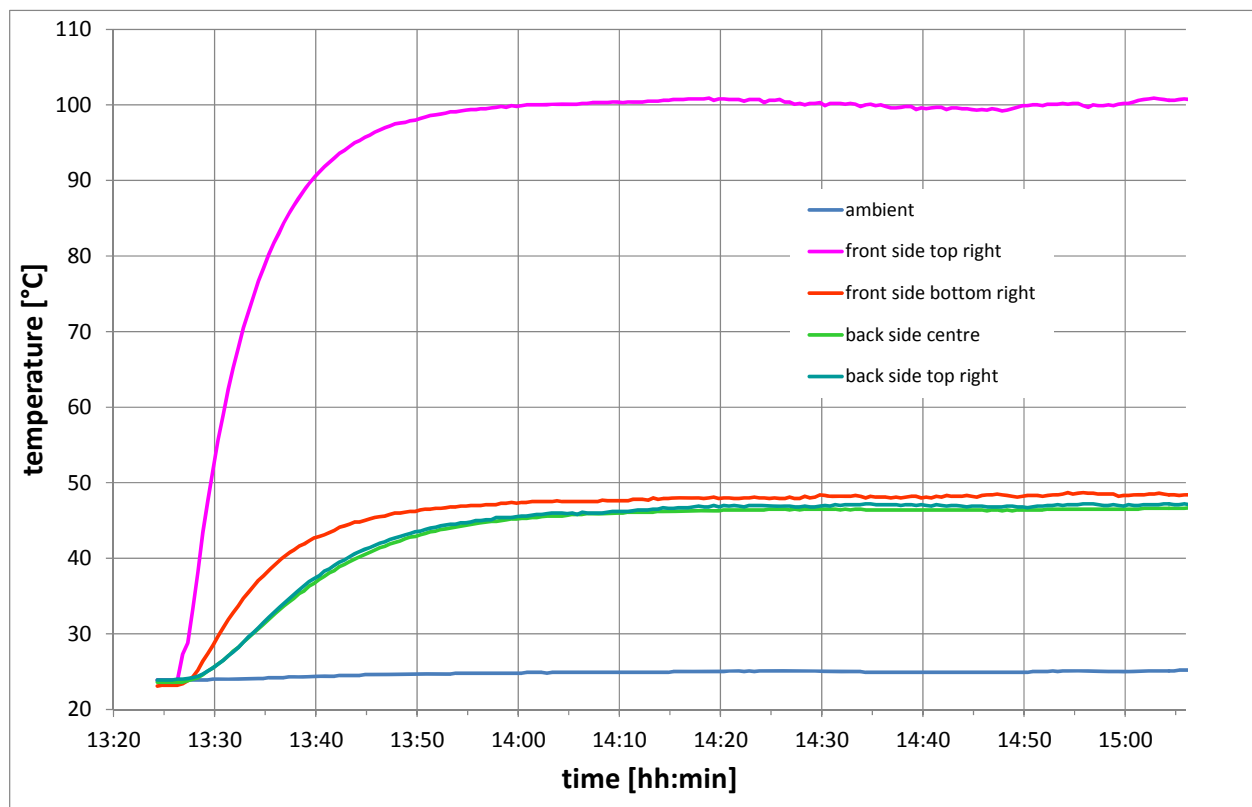


Figure 4: Temperatures of the 4 temperature measuring points and the ambient air

5 Determination of the surface temperature of the infrared radiator using infrared thermography

Several thermography pictures were taken from the front and back side with and without thermocouples. All pictures show the same temperature distribution with slightly different surface temperatures due to fluctuation of the supply voltage.

The radiation heater shows on the front side at approx. $\frac{3}{4}$ of its height left and right from the middle the maximum temperature during operation. The lowest temperature during operation can be observed in the lower half of the back side.

Front side

For the calculation of the surface temperature the emissivity measured at the beginning was entered in the evaluation software.

For the emissivity of the front side of the radiation heater $\varepsilon = 0.96$ was used.

Figure 5 shows the thermography of the heater after 1 h 45 min of operation. The display range reaches from 38 °C to 102 °C.

The black frame shows the background of the radiation heater which is the backside of the room the picture was taken. Since the wall temperature of the room is with approx. 27 °C is below the display range it is displayed in black. Around the radiation heater a thin blue frame can be observed which represents the circumferential fold of the steel plate.

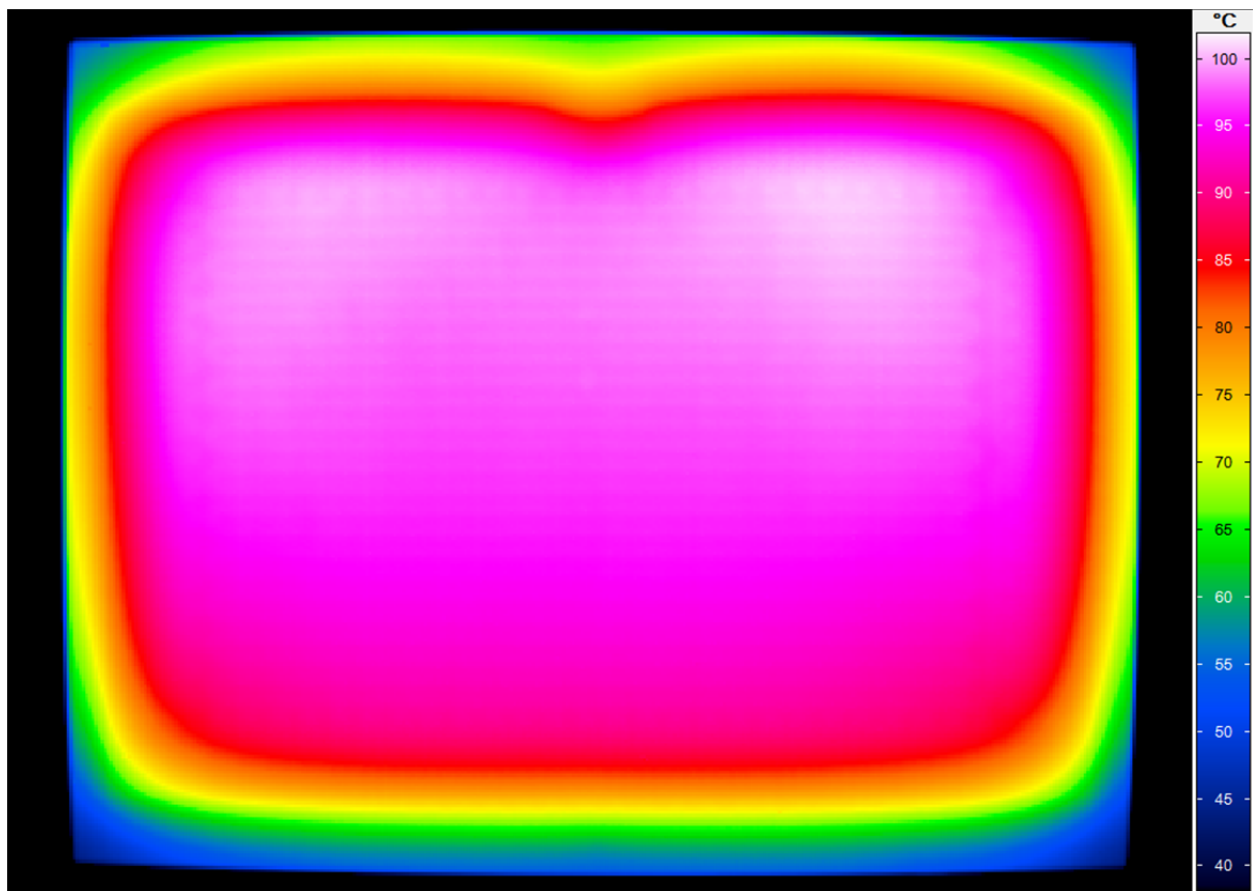


Figure 5: Thermography of the radiation heater, front view, display range 38 °C to 102 °C

The position of the steel cap at the back side is not visible from the front side. This shows that the steel plate at the front results in a very good temperature distribution.

The area displayed in red-orange with temperatures of approx. 85 °C shows a kind of valley at the top in the middle. At this position the mains supply is connected.

Altogether, due to free convection, the top half of the radiation heater has an approx. 7 K higher temperature than the lower half.

Figure 6 shows the thermography divided into 10 subareas. The display range is in the range of 29 °C to 100 °C. Due to the slight pillow like distortion of the lens a small part of the edge cannot be used for the calculation of the minimum and mean temperature of the surface. However, with respect to the following consideration of the radiation power this effect can be neglected.

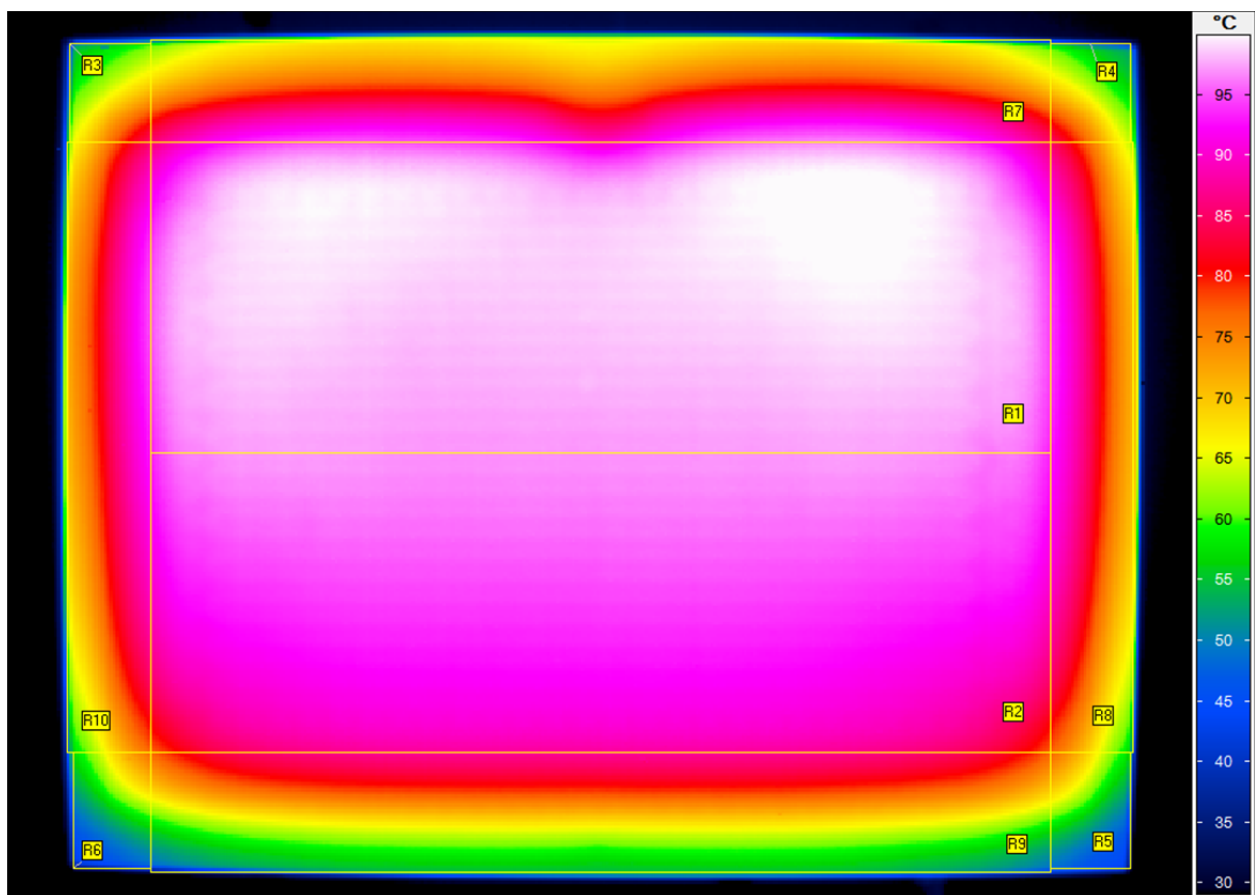


Figure 6: Thermography of the radiation heater, front side, with subareas, display range 29 °C to 100 °C

In table 1 the minimum, maximum and mean temperatures of the subareas are shown. As expected the two lower edges (see R5 and R6) show the lowest temperatures. The top interior subarea (R1) represents 31.4 % of the total area and shows a mean temperature of 98.1 °C. The highest temperature reaches 101 °C.

The mean temperature of the front side of the radiation heater is 87.5 °C at an electrical power consumption of 580 W, an ambient air temperature of 24 °C and a mean temperature of the surrounding surfaces (walls without back side, ceiling, floor) of 23 °C.

subarea	area ratio in %	mean in °C	minimum in °C	maximum in °C
R1	31.35	98.08	85.0	100.91
R2	30.44	93.13	76.78	97.41
R3	0.86	65.68	41.72	85.24
R4	0.97	64.49	39.32	85.0
R5	1.13	55.75	29.48	77.09
R6	1.00	55.49	29.78	76.78
R7	10.35	79.45	44.18	96.74
R8	5.92	79.54	39.44	94.44
R9	12.54	69.56	31.12	87.56
R10	5.50	79.83	44.95	95.03

Table 1: Ratio of the subareas, minimum, maximum and mean temperatures of the different subareas

Back side

For the back side of the radiation heater also an emissivity of $\varepsilon = 0.96$ was used.

The thermography of the backside of the radiation heater is shown in figure 7. The display range reaches from 34 °C to 71 °C. The corresponding photograph is shown in figure 8. The radiation heater was installed with the delivered installation kit on a rig with two vertical L-profiles. Thereby parts of the backside were covered. The installation kit and the L-profiles have a temperature very close to ambient temperature and a low emissivity. Thus they are displayed in black on the thermography. At the four corners and in the middle of the lower edge of the heater altogether 5 small dark blue spots are visible. At the positions of the small spots the screws are located which connect the front steel plate with the back wall. Since the emissivity of uncoated metal is very small and the temperatures of the whole area were calculated using an emissivity of 0.96 the temperatures of the screw heads in figures 7 and 9 show a temperature which is much lower than the real temperature. In addition 4 larger dark blue spots are visible in the corners. These are the positions of the spacers made from plastics. In the middle of the top edge the product label, as well as the cap of the electrical power supply and the connecting cable are placed.

Circling the edge which is not covered from the steel cap the highest temperatures up to 69 °C are found. The thermal conductivity of the steel plate, benefitted by the direct contact between the cap and the front plate, results in relatively high temperatures of the edges of the cap.

In the centre of the back side the surface temperature reaches 46 °C.

To determine the mean temperature of the back side the area was subdivided in the subareas R1 to R10 as shown in figure 9. The mean temperature of these subareas was calculated using the evaluation software of the thermography camera. The area covered by the installation kit and the connecting cable was subdivided in 7 additional areas (R11 to R17). The mean temperatures for these subareas were calculated using the mean values of adjacent subareas or several single temperatures at the edges of the subareas. Using all mean values a weighted mean value was calculated for the surface temperature of the back side. Measured values and calculated values (cursive) are listed in table 2.

Under the same boundary conditions as for the thermography of the front side **the mean surface temperature of the backside is 46.1 °C.**

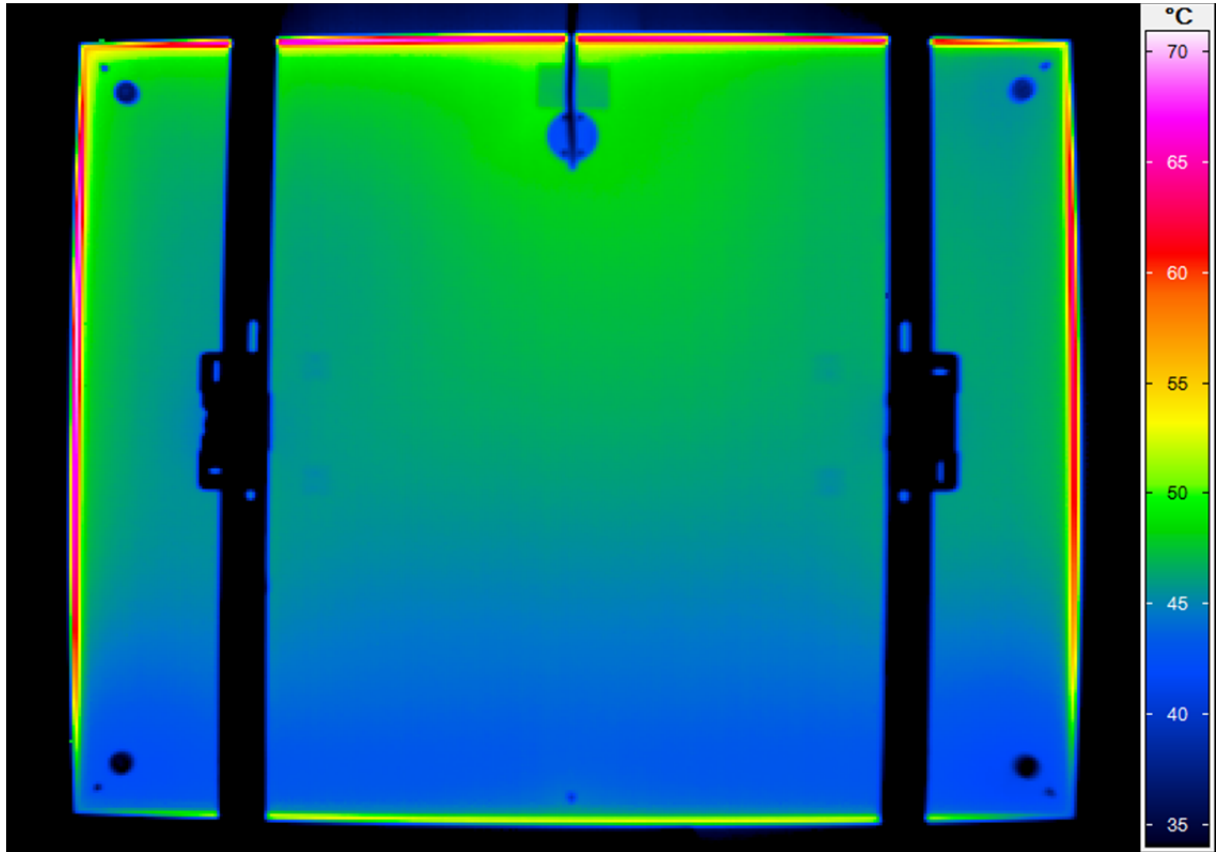


Figure 7: Thermography of the radiation heater, back view, display range 34 °C to 71 °C



Figure 8: Picture of the radiation heater, back view, with installation kit and connecting cable

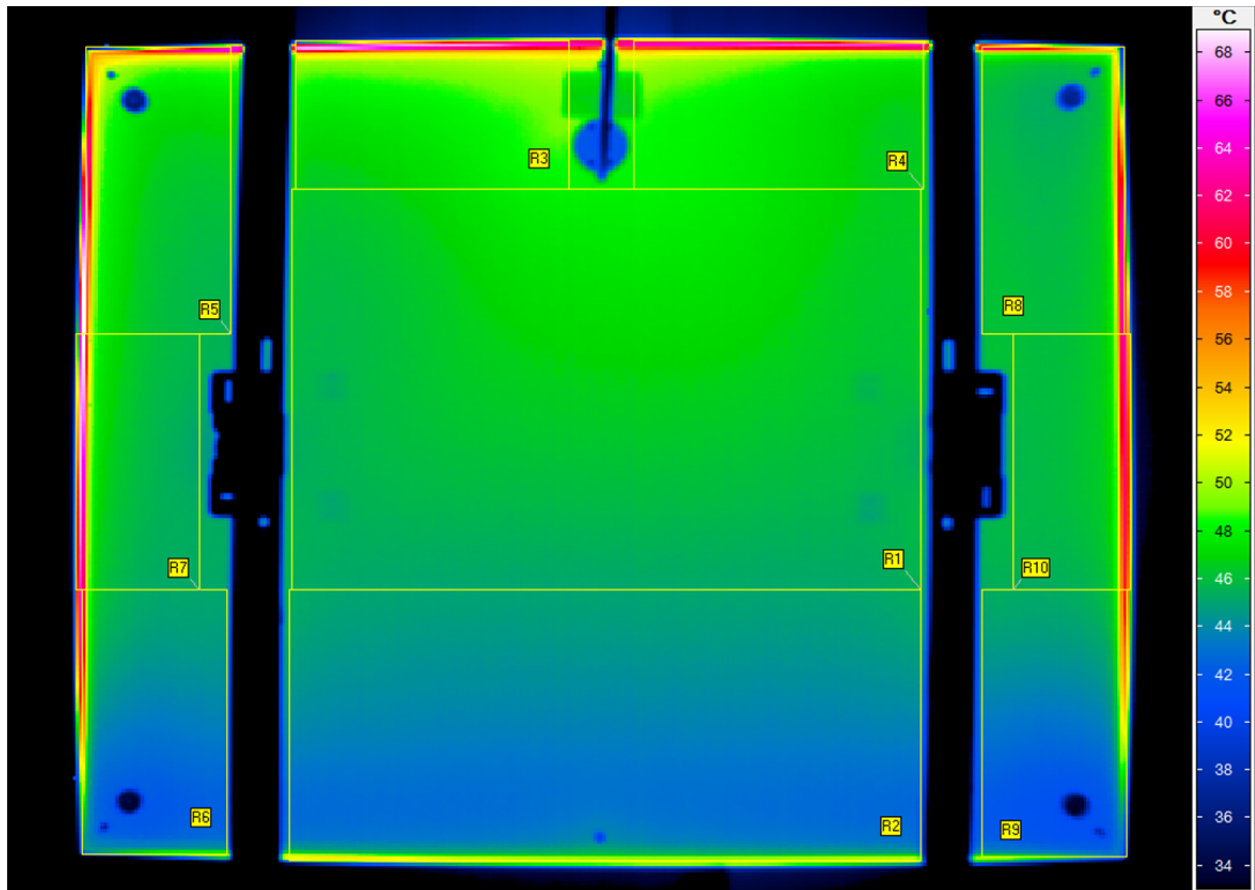


Figure 9: Thermography of the radiation heater, back view, with subareas, display range 33 °C to 69 °C

subarea	area ratio in %	mean in °C	minimum in °C	maximum in °C
R1	29.37	46.26	44.93	48.13
R2	19.98	44.06	39.72	52.33
R3	4.77	49.27	41.98	67.74
R4	5.00	48.74	46.44	66.31
R5	4.89	47.91	34.79	67.50
R6	4.68	44.01	33.44	61.04
R7	4.04	47.56	44.85	69.28
R8	4.79	46.86	33.22	63.52
R9	4.58	43.83	33.18	59.92
R10	3.49	47.38	43.28	63.27
R11	1.12	49.0	-	-
R12	2.10	48.5	-	-
R13	2.05	44.0	-	-
R14	2.48	46.3	-	-
R15	1.98	47.7	-	-
R16	1.93	43.9	-	-
R17	2.76	46.2	-	-
R1 – R17	100	46.09	-	-

Table 2: Ratio of the subareas, minimum, maximum, mean temperatures of the different subareas and mean temperature of the backside

6 Calculation of the radiation fractions of the infrared radiator

The fractions of the radiation emitted by the radiation heater in the different wavelength intervals were calculated using the radiant power in these wave length intervals. The radiant power was calculated using the Planck radiation law, the emissivity and the mean temperature of the surface of the front side:

$$M = \int_{\lambda_u}^{\lambda_o} \frac{\varepsilon c_1}{\lambda^5 \left(e^{\frac{c_2}{\lambda T}} - 1 \right)} d\lambda$$

With:

Radiant power M in W/m²

Radiation constant C₁ = 3.741775 * 10⁻¹⁶ W*m²

Radiation constant C₂ = 1.43877 * 10⁻² K*m

Emissivity ε: 0.96

Absolute temperature of the surface T: 87.47 °C + 273.15 K = 360.62 K

Wave length λ: IR-A 0.78 μm – 1.4 μm, IR-B 1.4 μm – 3.0 μm, IR-C 3,0 μm – 1000 μm

Table 3 shows the results for the calculation for the fractions of the radiation.

99.9 % of the radiated power is emitted in the wavelength range IR-C, and hence between 3.0 μm and 1000 μm.

	M(IR-A)	M(IR-B)	M(IR-C)	M _{tot}
Radiant power (W/m ²)	~ 0	~ 0.7	~ 920.0	~ 920.7
Radiation fraction (%)	~ 0	~ 0.1	~ 99.9	100

Table 3: Absolute radiant power and radiation fraction of the radiation heater for different wave length ranges

7 Calculation of the radiated power, the radiated efficiency and the heat emitted by free convection

The emitted net radiation of a surface which is in radiation exchange with the surrounding surfaces is calculated using the following equation:

$$\dot{Q}_{12} = A_1 * \sigma * (T_1^4 - T_2^4) / [(1/\varepsilon_1) + (1/\varepsilon_2 - 1) * A_1/A_2]$$

With:

A_1 = emitting subarea of the radiation heater ($R1_{\text{vorne}} - R10_{\text{vorne}}$ and $R1_{\text{hinten}} - R17_{\text{hinten}}$ respectively)

A_2 = surrounding area, walls without back side, ceiling and floor

ε_1 = emissivity of the radiation heater: 0.96

ε_2 = emissivity of the surrounding surfaces: 0.90 (determined with thermography camera)

T_1 = absolute temperature of the surface of the radiation heater, subareas see above

T_2 = absolute temperature of the surrounding surfaces: 296.15 K

σ = Stefan-Boltzmann-constant: $5.67 * 10^{-8} \text{ W}/(\text{m}^2\text{K}^4)$

For the calculation the same boundary conditions and measurement data have been used as for the thermography. The radiant power was determined separately for each subarea and the front and back side using the corresponding mean temperature (see table 1 and 2).

The radiant power of the front side is 320 W.

The radiant power of the back side is 92 W.

The radiant efficiency is calculated as followed:

$$\eta_{\text{radiant}} = \frac{\dot{Q}_{\text{radiant}}}{P_{\text{electric}}} * 100 \%$$

At an electrical power consumption of the radiation heater of 580 W the radiation efficiency of the front side is 55 % and in a total radiation efficiency, taking the front and back side into account, is 71 %.

Electrical heaters of this type convert all the supplied electric power into heat. Due to the punctual contact at the backside to the installation kit a heat transfer by heat conduction can be neglected. Thus the heating power transferred by natural convection can be calculated as following:

$$\dot{Q}_{\text{convection}} = P_{\text{electric}} - \dot{Q}_{\text{radiant}}$$

At an electrical power consumption of the radiation heater of 580 W the **heating power transferred by free convection is 168 W** or 29 % respectively.

8 Test methods

The determination of the emissivity was carried out with the Emissiometer 2000 (temperature 70 °C) of the measuring system OPTOSOL.

For the thermography the thermography system VarioCAM® high resolution and the software IRBIS® 3 plus were used.

The measurement of the electrical power consumption was carried out with the measuring device IME Tema fp.

Arrival of test sample: 18.05.2016

Arrival of coated samples: 23.05.2016

Test period: 22.06.2016 – 13.07.2016

Test engineer: Dipl.-Ing. (FH) C. Twerdy

Stuttgart, den 25.07.2016



Dr.-Ing. Harald Drück
Head of TZS